Characteraction of Ag-doped ZnO thin film synthesized by sol–gel method and its using in thin film solar cells

Fenglin Xian *, Kaibo Miao, Xuecheng Bai, Yun Ji, Feier Chen, Xiangyin Li

Department of Applied Physics, Nanjing University of Science and Technology, Nanjing 210094, China

ABSTRACT

Pure 2% and 4% Ag-doped ZnO thin films have been synthesized on glass substrates by sol–gel method. The structure, morphology and optical properties of the samples have been studied by X-ray diffractometer (XRD), scanning probe microscope, UV–vis spectrophotometer, respectively. The XRD result shows that the pure ZnO has a wurtzite hexagonal structure, no phase segregation is observed. The surface morphology of pure ZnO thin film shows that the grains are growing preferentially along the *c*-axis orientation perpendicular to the substrates. The transmittance spectra reveal that all samples have high transmittance above 90% in visible region. With Ag doping content increase, a red shift is observed. The performance of Ag-doped ZnO films using in thin film solar cells are simulated. The results show that 4% Ag-doped ZnO thin film can greatly improve the absorption of the cells. Compare to pure ZnO, solar cell's energy conversion efficiency improvement of 2.47% is obtained with 4% Ag doped ZnO thin film.

© 2013 Elsevier GmbH. All rights reserved.

1. Introduction

Zinc oxide, as an important semiconductor material, with a wide band gap energy of 3.37 eV, high exciton binding energy of 60 meV, a wide range resistivity, high electron Hall mobility ($200\,cm^2\,V\,s^{-1}$) and high transparency at room temperature [1]. These unique properties make ZnO have many potential applications, such as ultraviolet (UV) photoconductive detectors [2], solar cells [3], photocatalysts [4], light emitting diodes [5], especially for solar cells. They have been growing research efforts to improve the cell efficiency by optical absorption. For example, Ko and Yu [6] synthesized Ag doped ZnO nanorod arrays and found that Ag incorporation can greatly increase the optical absorption. Moreover, ZnO is a cheap, abundant, chemically stable and no toxin material with excellent radiation hardness. Various techniques have been applied to prepare ZnO thin films. For example, RF magnetron sputtering [7], chemical vapor deposition (CVD) [8], molecular beam epitaxy (MBE) [9], electrochemical deposition [10], pulse laser deposition (PLD) [11] and sol–gel method [12] are widely used. Among these techniques, sol–gel method attracts much attention due to some unique advantage including low cost, simple deposition equipment, easy adjusting composition and dopants, and fabricating large area films.

In this article, Ag-doped ZnO thin films with various doping concentration are prepared by sol–gel method. The structure, optical transmittance, electronic property and its using as solar cell's windows material are investigated.

2. Experiment

Ag-doped ZnO films were synthesized via sol–gel method. Commercially available zinc acetate 2-hydrate was dissolved in anhydrous ethanol to form ZnO solution. Ethanolamine was used as stabilizer. The total concentration of metal ions was maintained at 0.3 mol/L and the molar ratio of ethanolamine to the total metal ions was 1:1. The Ag doping ratio defined by [Ag]/[Ag + Zn] varied over a range of 0–4%. Before adding dopant, the pure ZnO solution was stirred for an hours at 60 °C. Then the mixture was stirred for two hour. The films were prepared by spin-coating method. The spin coating speeds were 1200 rpm for the first 10 s and 3000 rpm for the next 20 s. After spin coating process, the samples were dried at 300 °C for 8 min to evaporate the solvent and organic residuals. The process of spin coating and subsequent pre-heating treatment was repeated several times to obtain a desired thickness. At last, all the samples were annealing at 500 °C for an hour in air.

The structure of Ag-doped ZnO thin films was studied by X-ray diffractometer (Bruker D8 Advance). The surface morphologies were observed by scanning probe microscope (CSPM4000). The transmittance spectrum of Ag-doped ZnO thin films were measured by UV-visible spectrophotometer (UV-1201). The current–voltage (*I*–*V*) curve was measured at dark and under UV light illumination using a high pressure mercury lamp (175 W).

* Corresponding author. Tel.: +86 25 84318547; fax: +86 25 84318547.
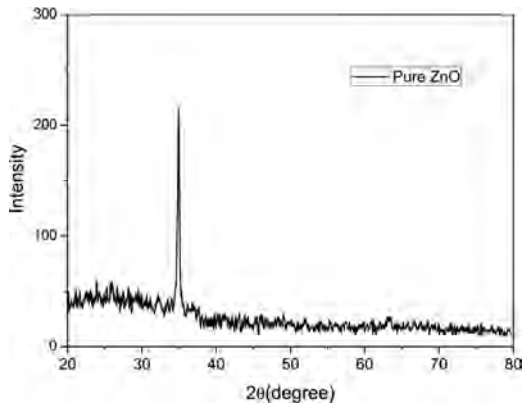*E-mail address:* xfl6880@sohu.com (F. Xian).

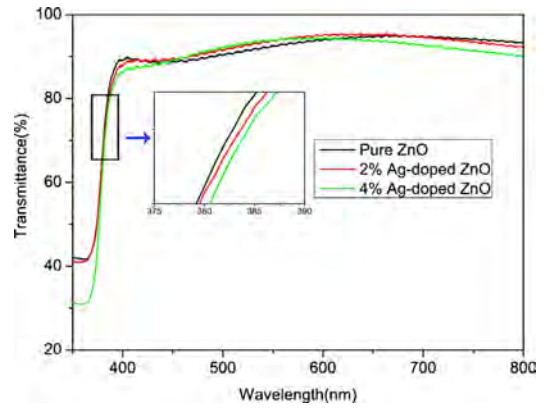**Fig. 1.** X-ray diffraction pattern of pure ZnO thin films.

Fig. 3. Transmittance spectra of pure, 2% and 4% Ag doped ZnO thin films.

3. Results and discussion

3.1. The structure, optical and electrical properties of the samples

Fig. 1 shows X-ray diffraction patterns of pure ZnO thin films. It can be seen that there is only one strong diffraction peak at 34.92 degree, which correspond to the (0 0 2) plane of ZnO with wurtzite hexagonal structure. The strong diffraction intensity and narrow full-width at half-maximum (FWHM) of the diffraction peak confirms that the ZnO is well crystallized.

The surface morphology of pure ZnO thin film measured by scanning probe microscope is illustrated in Fig. 2. The 2D and 3D atom force microscope (AFM) images are showed in Fig. 2(a) and (b), (c) and (d) show the grain diameter distribution and height distribution. It exhibits that all samples have dense grains. The grains are growing preferentially along the c-axis orientation perpendicular to the substrates. The average grain size is about 200 nm and the height is about 60 nm. Besides, a few sharp columns are observed on the surface of the film. This may due to the reunion and growth of grains during the annealing process.

The transmission spectra of pure, 2% and 4% Ag doped ZnO thin films are measured by ultraviolet visible spectrophotometer. The transmission spectra of all the samples are shown in Fig. 3. It can be seen that all three samples have sharp absorption peaks at around 370 nm in ultraviolet region which represent intrinsic absorption peaks of ZnO. Compare to pure and 2% Ag-doped ZnO, the absorption is greatly increased by 4% Ag doping. The transmittance of all samples in visible region is about 90%. There is no obvious changing with Ag doped. From the enlarge area of the absorption band edges in the inset. It can be seen that with Ag doping concentration
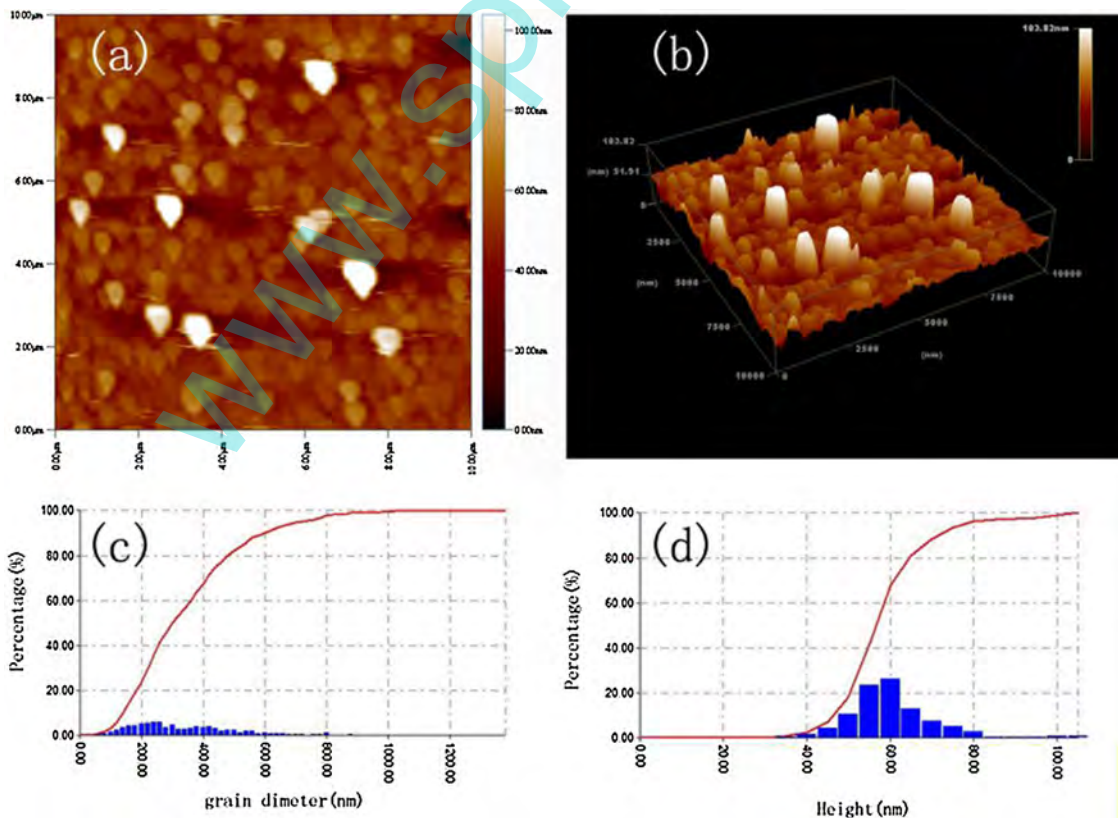

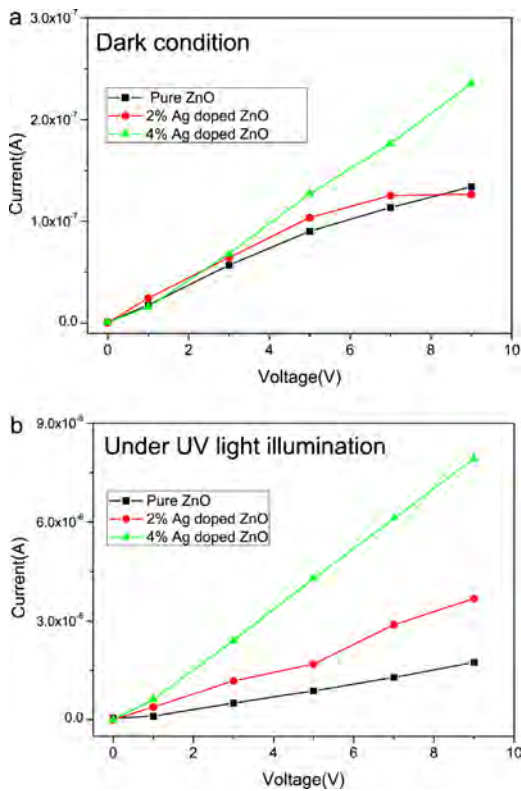**Fig. 2.** AFM image of pure ZnO thin film.

Fig. 4. (a) I–V curve of pure, 2% and 4% Ag doped ZnO thin films under dark condition. (b) I–V curve of pure, 2% and 4% Ag doped ZnO thin films under UV light illumination.

increases, the absorption band edge is shifted to long wavelength. The red shift demonstrates that the band gap of ZnO decreases with Ag doping density increases.

Fig. 4 shows the current–voltage curves of pure, 2% and 4% Ag doped ZnO thin films under dark and UV light illumination (ultraviolet high pressure mercury lamp, 175 W). Under dark condition, it can be seen that the current magnitude all three samples is 10^{-7} A, and increases with increasing applied voltage. When doping density of Ag is increasing, the current becomes larger and rise most rapidly while the Ag doping density is 4%. It is because the conductivity of ZnO is improved with the incorporation of Ag ions. Under the UV light illumination, the current of all samples increases up to a magnitude of 10^{-6} A. Compare the photocurrent with the current under dark condition. One can infer that all samples have strong UV response characteristics. 4% Ag-doped ZnO thin film exhibits a stronger light response than pure and 2% Ag-doped ZnO thin films. This is attributed to that a proper Ag doping (4%) can greatly enhance the separation of electron–hole pairs.

3.2. Solar cells simulation

In this article, the solar cells simulation is based on RCWA method, which is a program based on rigorous coupled-wave theory (RCWT) to analyze and design diffractive structures. It is a rigorous solution of Maxwell's equations with corresponding boundary conditions for the electromagnetic diffraction properties by periodic grating structures. And now we have applied the RCWA for calculating the optical absorption of solar cell devices.

We build the coupled wave equations in each layer, and after that, utilize electric and magnetic field boundary continuity conditions to connect the electric and magnetic field of all layers depending on the coupled wave equations. Finally, we can get the total reflectance R and transmittance T of the solar cells. The absorbance A can be calculated by $A = 1 - R - T$ [13].
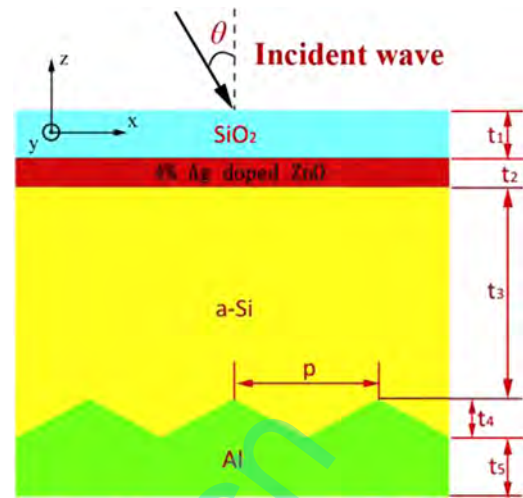

Fig. 5. The solar cell's schematic structure.

The solar cell's schematic structure is shown in Fig. 5. A thin layer of Ag-doped ZnO thin films coated on the glass is acted as the top transparent electrode and the antireflection coating. The active layer is a-Si. The back aluminum triangle structure is used as blazed gratings. The optimized geometrical parameters of the structure are obtained by RCWA simulations performed for each set of parameters. The thickness of glass $t_1 = 50$ nm, while the Ag-doped ZnO layer $t_2 = 20$ nm. The thickness of the active layer $t_3 = 400$ nm, and the back blazed grating's height $t_4 = 40$ nm, period $p = 150$ nm. The plate part's thickness $t_5 = 50$ nm (Fig. 6).

Fig. 4 shows the total absorption of thin films solar cell with various Ag-doped ZnO layers. It can be seen that in the wavelength region from 0.65 μm to 1.1 μm, there is no obvious changing among pure, 2% and 4% Ag-doped ZnO thin films. But in the wavelength region of 0.35–0.6 μm, the device with 4% Ag-doped ZnO layer has higher absorption than others, especially in UV region. This is well matching the experimental results. The solar cell efficiency is calculated by:

$$\eta = \frac{J_{SC} V_{OC} FF}{P_{in}} \tag{1}$$

where J_{SC} is the short-circuit density, V_{OC} is the open-circuit voltage, FF is the filling factor, and P_{in} is the total incident power and is defined as:

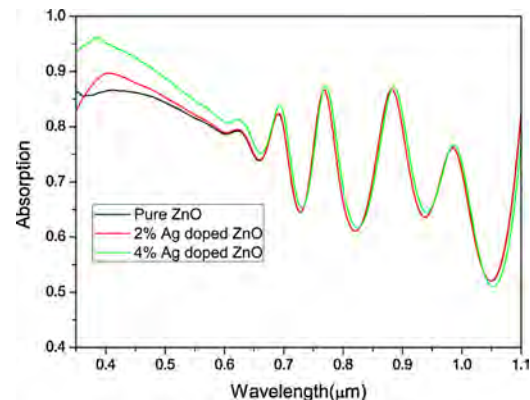$$P_{in} = \int S(\lambda) d\lambda \tag{2}$$

Fig. 6. The absorption of the solar cell device.

Table 1
The calculated parameters of the device.

Samples	V_{OC} (V)	FF	J_{SC} (A/m^2)	η (%)
ZnO	0.791231	0.859305	−294.15	28.1416
2% Ag doped ZnO	0.791332	0.859318	−295.3	28.2557
4% Ag doped ZnO	0.791839	0.859386	−301.147	28.8359

where $S(\lambda)$ is the incident spectrum of a standard AM1.5 solar spectrum. The calculated parameters of the device, including cell efficiency (η), filling factor (FF), open circuit voltage (V_{OC}) and short circuit current (J_{SC}), are illustrated in Table 1. It can be seen that Ag doping can effectively improve the performance of the device. Compare to the device with pure ZnO, a improvement of 2.47% of the device with 4% Ag-doped ZnO layer was obtained.

4. Conclusion

Pure, 2% and 4% Ag-doped ZnO thin films have been successfully synthesized on glass substrates by sol–gel method. The structure, morphology and optical properties of the samples have been studied by X-ray diffractonmeter (XRD), scanning probe microscope, UV–vis spectrophotometer, respectively. The XRD result shows that the pure ZnO has a wurtzite hexagonal structure, no phase segregation is observed. The surface morphology of pure ZnO thin film shows that the grains are growing preferentially along the c-axis orientation perpendicular to the substrates. The transmittance spectra reveal that all samples have high transmittance above 90% in visible region. There is no obvious changing with Ag doping. With Ag doping content increase, a red shift is observed. The performance of Ag-doped ZnO films using in thin film solar cells are simulated. Compare to pure ZnO, 4% Ag-doped ZnO thin film can greatly improve the absorption of the cells. Energy conversion efficiency improvement of 2.47% is obtained with 4% Ag doped ZnO thin film.

References

[1] S.J. Pearton, D.P. Norton, K. Ip, Y.W. Heo, T. Steiner, Recent advances in processing of ZnO, J. Vac. Sci. Technol. B 22 (2004) 932–948.
[2] J. Sun, Q. Dai, F. Liu, H. Huang, Z. Li, X. Zhang, Y. Wang, The ultraviolet photoconductive detector based on Al-doped ZnO thin film with fast response, Sci. China. Phys. Mech. Astron. 54 (2011) 102–105.
[3] Gonzalez-Valls, M. Lira-Cantu, Vertically-aligned nanostructures of ZnO for excitonic solar cells: a review, Energy Environ. Sci. 2 (2009) 19–34.
[4] J. Xia, A. Wang, X. Liu, Z. Su, Preparation and characterization of bifunctional, Fe$_3$O$_4$/ZnO nanocomposites and their use as photocatalysts, Appl. Surf. Sci. 257 (2011) 9724–9732.
[5] S.W. Lee, H.D. Cho, G. Panin, T.W. Kang, Vertical ZnO nanorod/Si contact light-emitting diode, Appl. Phys. Lett. 98 (2011) 093110 (1–3).
[6] Y.H. Ko, J.S. Yu, Optical absorption enhancement of embedded Ag nanoparticles with ZnO nanorod arrays, Phys. Status Solidi (a) 208 (2011) 2778–2782.
[7] J.S. Cho, Y.J. Kim, J.C. Lee, S.H. Park, K.H. Yoon, Structural and optical properties of textured ZnO:Al films on glass substrates prepared by in-line rf magnetron sputtering, Sol. Energy Mater. Sol. Cells 95 (2011) 190–194.
[8] K. Tang, S.L. Gu, S.Z. Li, J.D. Ye, S.M. Zhu, H. Chen, J.G. Liu, R. Zhang, Y. Shi, Y.D. Zheng, Influence of thermally diffused aluminum atoms from sapphire substrate on the properties of ZnO epilayers grown by metal-organic chemical vapor deposition, J. Vac. Sci. Technol. A 29 (2011) 03A106 (1–7).
[9] A.S.H. Hussein, Z. Hassan, S.M. Thahab, S.S. Ng, H. Abu Hassan, C.W. Chin, Effect of Al mole fraction on structural and electrical properties of Al$_x$Ga$_{1-x}$N/GaN heterostructures grown by plasma-assisted molecular beam epitaxy, Appl. Surf. Sci. 257 (2011) 4159–4164.
[10] D.Q. Gao, D.S. Xue, Y. Xu, Z.J. Yan, Z.H. Zhang, Synthesis and magnetic properties of Cu-doped ZnO nanowire arrays, Electrochim. Acta 54 (2009) 2392–2395.
[11] O.A. Novodvorsky, L.S. Gorbatenko, V.Y. Panchenko, O.D. Khramova, Y.A. Cherebilo, C. Wenzel, J.W. Bartha, V.T. Bublik, K.D. Shcherbachev, Optical and structural characteristics of Ga-doped ZnO films, Semiconductors 43 (2009) 419–424.
[12] B.K. Sonawane, M.P. Bhole, D.S. Patil, Structural, optical and electrical properties of MgxZn$_{1-x}$O ternary alloy films, Mater. Sci. Semicond. Process. 12 (2009) 212–216.
[13] M.G. Moharam, D.A. Pommet, E.B. Grann, T.K. Gaylord, Stable implementation of the rigorous coupled-wave analysis for surface-relief gratings: enhanced transmittance matrix approach, J. Opt. Soc. Am. A 12 (199) (1995) 1077–1086.